DEFECT CHARACTERIZATION IN CERAMICS USING HIGH FREQUENCY ULTRASONICS

G. S. Kino, B. T. Khuri-Yakub, Y. Murakami, and K. H. Yu
Stanford University
Stanford, California 94305

ABSTRACT

A high frequency A-scan system (150-450 MHz longitudinal, 150-300 MHz shear) has been used to characterize defects in ceramics. An Indium bonding technology has been developed to make broadband, and efficient transducers. Defect characterization is done by comparing the time domain backscattered signals from defects to theory. A Wiener filter is used in order to correct the response of the transducer and the propagating medium, and thus give the impulse response of real defects. A good agreement between theory and experiment is obtained for inclusions such as voids, WC, and SiC in Si_3N_4.

INTRODUCTION

Ceramic materials such as Si_3N_4 and SiC are becoming increasingly important structural materials because of their high strength, and high temperature capabilities. However, because ceramic materials are brittle, it is important to detect small inclusions in the size range of 10 - 100 μm. For this purpose we design our A-scan system to operate in the frequency range of 150 - 500 MHz with longitudinal wave transducers and in the range of 150 - 300 MHz with shear wave transducers.

In this work we describe pulse echo techniques and backscatter measurements as a function of frequency conducted on flaws in ceramics (Si_3N_4). We are concerned with comparing the reflected echo signals to theoretical calculations of scattering from flaws as a function of frequency. Alternatively, we are interested in the backscattered signal as a function of time due to an incident narrow acoustic base band pulse, which at least in theory has the form of a δ function.

We describe, in this paper how we have used Wiener filtering techniques to correct for the transducer response variation as a function of frequency and obtain after processing very narrow pulses. We correct not only for defects in the transducer characteristic itself, but also for distortion of the signals by the contacting system employed and by the attenuation in the sample varying with frequency. By this means we can use the corrected pulse to probe a flaw and the output signal obtained shows the true time domain response from the flaw, which can then be compared to theory. Experimental results obtained with real defects such as WC in Si_3N_4, and vacancies in Si_3N_4 are presented and used to predict the type and size of the defects.

The transducers used in our work were originally made by rf sputtering an 8 μm thick zinc oxide (ZnO) film on a sapphire ($A\ell_2O_3$) buffer rod.[1] The transducers thus obtained are longitudinal wave transducers resonant at a center frequency of 300 MHz. In order to achieve more efficient, and broadband transducers, we developed an Indium (In) bonding technology.[2] With In bonding, we can use single crystal piezoelectric materials such as Lithium Niobate ($LiNbO_3$), and we can make either longitudinal or shear wave transducers. A schematic diagram of an In bonded transducer is shown in Fig. 1. The Titanium (Ti) and Gold (Au) layers are first evaporated on the surfaces to be bonded. The samples are then placed in a vacuum station where In is evaporated, and the surfaces pressed against each other with a pressure of 500 kg/cm^2, without breaking the vacuum. The In and Au form an alloy which makes a very strong cold bond. The piezoelectric material is then polished to the desired thickness for operation in the frequency range of interest. The impulse of an In bonded, $LiNbO_3$ on Silicon Nitride (Si_3N_4) shear wave transducer is shown in Fig. 2. The untuned two-way insertion loss of the transducer of Fig. 2 is shown in Fig. 3. A loss of 4 dB is due to diffraction, and propagation loss in the Si_3N_4 buffer rod.

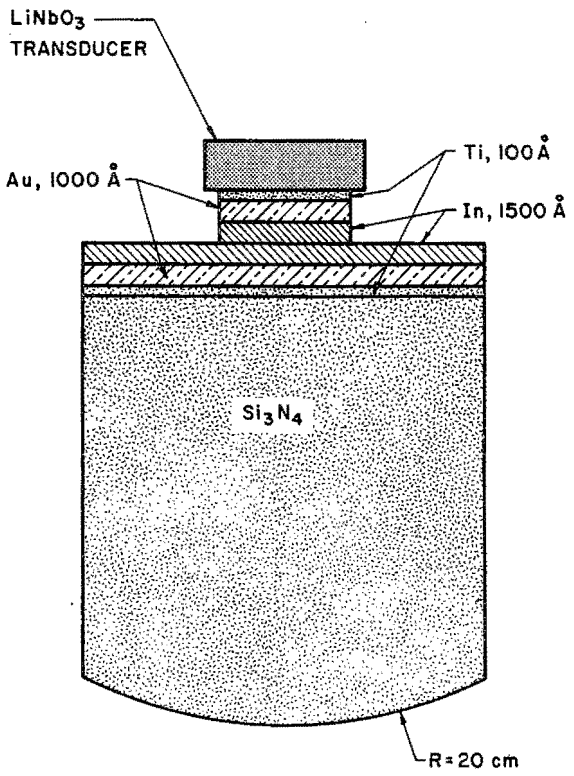

Fig. 1. Schematic diagram of Indium bonded transducer.

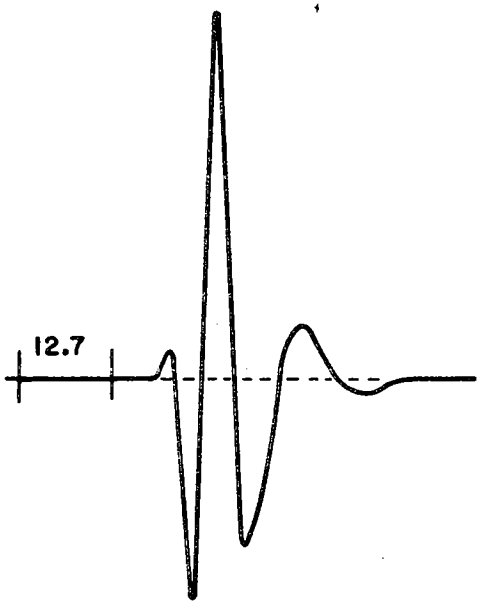

THEORETICAL IMPULSE RESPONSE

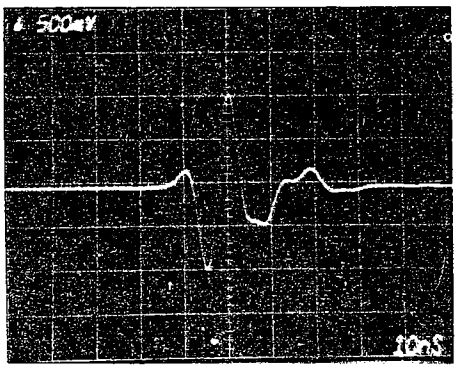

Fig. 2. Impulse response of $LiNbO_3/Si_3N_4$ shear wave Indium bonded transducer.

A schematic diagram of the A-scan system used in our study is shown in Fig. 4. The bottom end of the buffer rod is polished with a radius of curvature of 20 cm. Contact to the ceramic under study is made by pushing the curved end of the buffer rod against the ceramic without using a contacting layer such as gold.[3] The transducer is excited with a 30 V, 2 nsec electric pulse in order to obtain broad bandwidth operation.

The received signal at the transducer is passed into a sampling oscilloscope which yields an output which is a slowed down version of the pulse, a Biomation analog-to-digital converter is used to sample the slowed down pulse and digitize it for insertion into a PDP 11-10 minicomputer. The computer is used to take fast Fourier transforms and correct the received signal.

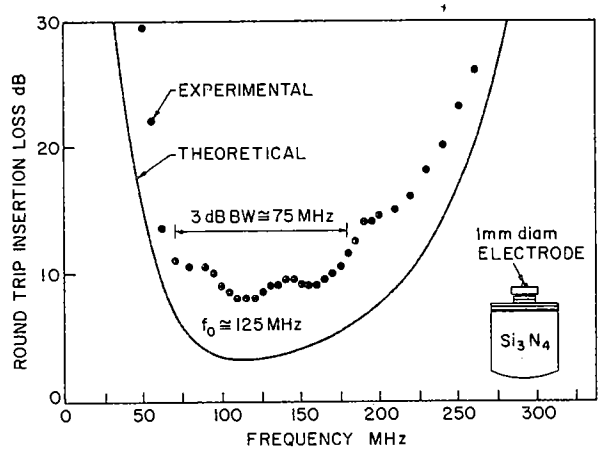

Fig. 3. Two-way insertion loss of a delay line with the transducer of Figs. 1 and 2.

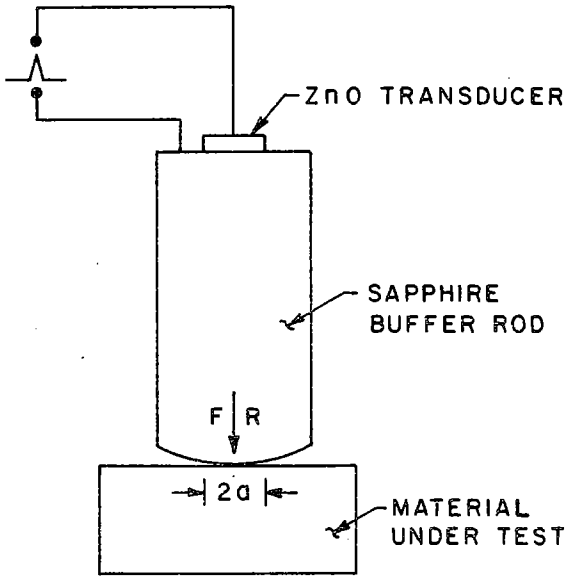

R = 20 cm
2a = .1 cm
F = 172 N ≅ 39 Lbs.

Fig. 4. Schematic of A-scan system.

The frequency response $X(\omega)$ of the transducer pulse is calculated by carrying out a 512 point Fast Fourier Transformation (FFT). Time and frequency responses to our transducer are shown in Figs. 5(a) and 5(b), respectively. Ideally we would like to correct the transducer response by constructing an inverse filter with a response $1/X(\omega)$. However, at frequencies where $X(\omega) \to 0$

the filter would not be realizable. Instead we have designed a Wiener filter with a response

$$W(\omega) = \frac{X^*(\omega)}{X(\omega)\,X^*(\omega) + N^2} \qquad (1)$$

where N^2 is the noise level in the system. In the computation we set N^2 at an arbitrary but constant level, for simplicity.

From the formula (1), it is apparent that the total bandwidth above the arbitrary noise level of the transducer is being used instead of the 3 dB bandwidth; thus we can utilize the 10 dB or even 20 dB bandwidth of the transducer, and considerably improve the depth resolution by this technique. It will be noted that if $X(\omega)X^*(\omega) \gg N^2$, $W(\omega) \to 1/X(\omega)$, i.e., the system behaves like an inverse filter.

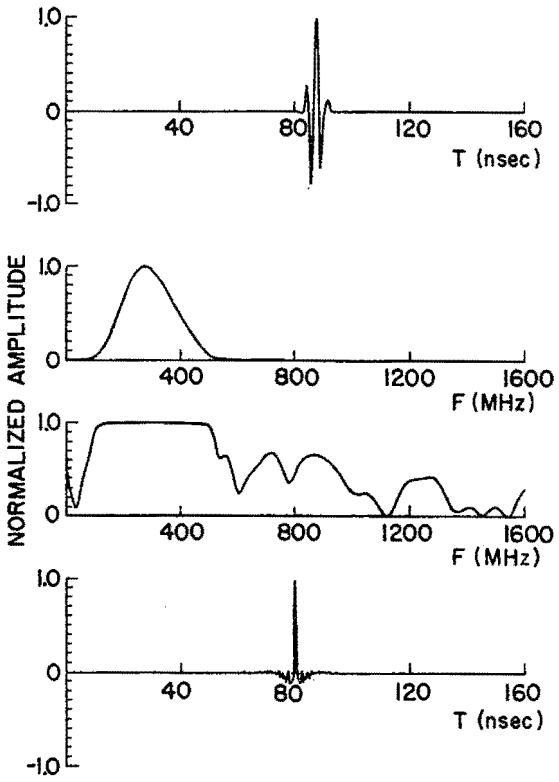

Fig. 5. Design of Wiener filter:
(a) Impulse response of $ZnO/A\ell_2O_3$ transducer.
(b) Frequency response of $ZnO/A\ell_2O_3$ transducer.
(c) Frequency response of $ZnO/A\ell_2O_3$ transducer after passing through the Wiener filter.
(d) Impulse response of $ZnO/A\ell_2O_3$ transducer after passing through the Wiener filter.

The output signal of the transducer pulse passed through this filter is calculated by multiplication in the frequency domain followed by the Inverse Fourier Transformation. As shown in Figs. 5(c) and 5(d) this output signal is uniform over a wide frequency range and is very close to a δ-function. Thus, we can effectively eliminate the defects in the transducer response, increase its effective bandwidth, and improve the impulse response and depth resolution by using a Wiener filter.

The picture in Fig. 6 shows the reflected pulse from an unknown defect in a silicon nitride ceramic. The adaptive filter technique was applied to the reflected signal in order to evaluate this defect. The output signal passed through the filter is shown in Fig. 7(a); its time domain response is compared with the theoretical response of a WC inclusion in Si_3N_4 shown in Fig. 7(b).

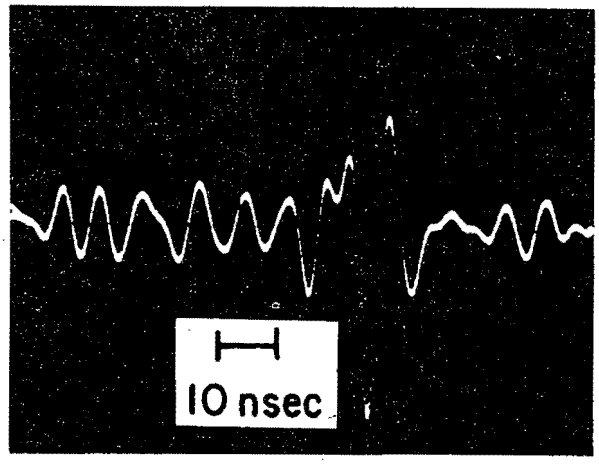

Fig. 6. Backscattered signal from an unknown inclusion in Si_3N_4.

Comparing Figs. 7(a) and (b), we conclude that the scattering from the unknown inclusion shown in Fig. 6 is equivalent to a WC sphere with a diameter of 90 μm. This result was obtained by measuring the delay between the front and back surface echoes in the time domain.

The normalized amplitude of the front surface echo from a spherical surface can be shown to have the following dependence[4]:

$$S_{11} \propto \frac{a\Gamma}{Z^2}$$

where a is the radius of the sphere, Γ is the reflection coefficient due to impedance mismatch, and Z is the distance from the transducer to the defect. By comparing the amplitude of the front surface echo to that of a hemispherical void drilled in the back of a piece of ceramic, we can make another estimate of the size of bulk defects. In the case of the defect shown in Fig. 6, we calculate a diameter of 100 μm. This result is in agreement with the size estimate from the time domain analysis.

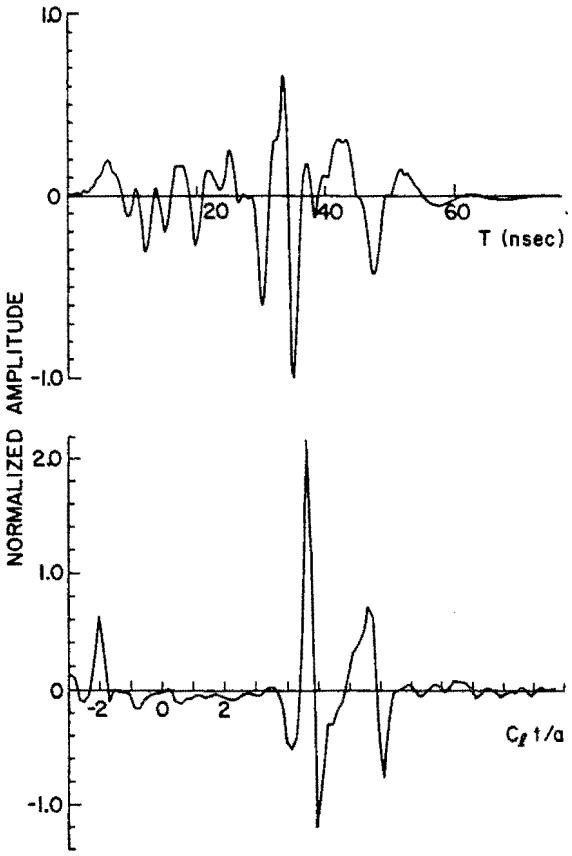

Fig. 7. Comparison of impulse responses in the time domain.
(a) Defect in Fig. 6.
(b) Theoretical WC inclusion.

The silicon nitride sample has been lapped down to the defect. The defect was found out at exactly the same location where we predicted, and its size was measured to be 160 μm diameter compared to our estimated 90 - 100 μm diameter. However the material within the defect has been analyzed by using X-ray spectroscopy, and turned out to be a two-phase mixture of Tungsten DiSilicide (WSi_2) and Silicon Carbide (SiC). Interestingly enough in our experimental time domain results shown in Fig. 7(a) there are extra peaks in the response between the two main pulses expected in the theory; this appears to be associated with the two-phase nature of the inclusion.

We note that our experimental measurement only gave a reasonable estimate of the size of the inclusion. But there was some error because the material of the inclusion had a higher velocity than expected for Tungsten Carbide. Thus we see that basically the technique determines the transit time of waves through the sample and the impedance mismatch at the sample. But other techniques such as low frequency angular scattering imaging measurements may be needed to supply one extra piece of information, the size or the density of the defect to allow all its parameters to be evaluated accurately.

A major advantage of the present technique over X-ray methods is that it very easily determines if the inclusion is in contact with the surrounding medium. Other samples of Tungsten Carbide in Silicon Nitride showed up in microfocus X-ray measurements, but behaved like vacancies acoustically. When they were lapped down, the Tungsten Carbide was found to be supported from the surrounding medium only by a small fillet.

Finally, this high frequency technique appears to yield information on the uniformity of the inclusion. In one case where a two-phase material was present, scattered signals from within the inclusion were clearly observed.

ACKNOWLEDGEMENTS

The work reported in this paper was supported by the Advanced Research Projects Agency through the U.S. Air Force under subcontract from Rockwell International under Contract RI74-20773.

REFERENCES

1. B. T. Khuri-Yakub and G. S. Kino, "Acoustic Pulse Echo Measurements at 200 MHz," Appl. Phys. Letters 30, 2 (15 January 1977).

2. C. Lardat, Thomson CSF, Cagnes-Sur-Mer, Private Communication.

3. S. Burns, J. Tien, B. T. Khuri-Yakub, and G. S. Kino, "Acoustic Coupling into an Elastic Solid by Hertz Contact Stresses," in press.

4. G. S. Kino, "The Application of Reciprocity Theory to Scattering of Acoustic Waves by Flaws," J. Appl. Phys. 49(6) (June 1978).